Magnesium-rich Intermetallics RE_3RuMg_7 (RE = Y, Nd, Dy, Ho) – Rows of Condensed Ru@$RE_{6/2}$ Octahedra in Magnesium Matrices

Marcel Kersting, Ute Ch. Rodewald, Christian Schwickert, and Rainer Pöttgen

Institut für Anorganische und Analytische Chemie, Universität Münster, Corrensstrasse 30, 48149 Münster, Germany

Reprint requests to R. Pöttgen. E-mail: pottgen@uni-muenster.de

Z. Naturforsch. **2013**, *68b*, 1273 – 1278 / DOI: 10.5560/ZNB.2013-3262
Received September 23, 2013

The magnesium-rich intermetallic phases RE_3RuMg_7 (RE = Y, Nd, Dy, Ho) have been synthesized from the elements in sealed niobium ampoules and subsequently characterized by powder X-ray diffraction. The structure of the dysprosium compound was refined on the basis of single-crystal X-ray diffractometer data: Ti_6Sn_5 type, $P6_3/mmc$, $a = 1019.1(2)$, $c = 606.76(9)$ pm, $wR2 = 0.0159$, 439 F^2 values, 19 variables. The Mg3 site shows a small degree of Mg3/Dy mixing, leading to the composition $Dy_{3.03}RuMg_{6.97}$ for the investigated crystal. The striking structural motifs in the Dy_3RuMg_7 structure are rows of face-sharing Ru@Dy_6 octahedra and corner-sharing Mg2@Mg_8Dy_4 icosahedra. The rows of octahedra form a hexagonal rod-packing, and each rod is enrolled by six rows of the condensed icosahedra. Temperature-dependent magnetic susceptibility measurements of Dy_3RuMg_7 show Curie–Weiss behavior with an experimental magnetic moment of 10.66(1) μ_B per Dy atom. Antiferromagnetic ordering is detected at $T_N = 27.5(5)$ K. The 5 K isotherm shows a metamagnetic transition at a critical field of $H_C = 40$ kOe.

Key words: Magnesium, Crystal Structure, Magnetic Properties, Dysprosium, Rare Earths, Ruthenium

Introduction

Among the large family of intermetallic magnesium compounds $RE_xT_yMg_z$ (RE = rare earth element, T = electron-rich transition metal) [1], only few with group VIII transition metals have been reported. $Ce_2Fe_2Mg_{15}$ [2] is the so far only iron-containing compound which crystallizes with its own structure type (a ternary ordered version of the Th_2Ni_{17} type). With ruthenium several series of isotypic compounds have been published. The rare earth-rich phases RE_4RuMg (RE = La–Nd, Sm, Gd–Ho) [3] and $RE_{23}Ru_7Mg_4$ (RE = La, Ce, Pr, Nd) [4] contain the rare structural motif of Mg_4 tetrahedra. The compounds RE_2RuMg_2 (RE = Dy, Ho, Er, Tm, Lu) [5] crystallize with a ternary ordered version of the Os_2Al_3 type, an i5 superstructure of the *bcc* packing. A similar situation is observed for the magnesium-rich phases RE_3RuMg_7 (RE = Sm, Gd, Tb) [6] which adopt a ternary ordered variant of the Ti_6Sn_5 structure.

Besides these series with several representatives each, also some singular structures have been observed. The $Nd_{4.67}Ru_3Mg_{8.83}$ structure [7] is built up from Ru@Mg_4Nd_4 square antiprisms and Mg@Mg_8 cubes as basic building units. $CeRu_2Mg_5$ [8] and $Ce_2Ru_4Mg_{17}$ [9] contain almost tetravalent cerium and exhibit extremely short Ce–Ru distances (232 respectively 231 pm), indicating strong covalent Ce–Ru bonding [10]. Due to the increased cerium oxidation state in $CeRu_2Mg_5$ and $Ce_2Ru_4Mg_{17}$, no isotypic compounds with the neighboring trivalent rare earth elements are known.

During our phase analytical studies of the RE-Ru-Mg systems we now obtained further members of the RE_3RuMg_7 series. The synthesis and structural characterization of RE_3RuMg_7 with RE = Y, Nd, Dy, and Ho are reported herein. Additionally we measured the magnetic properties of Dy_3RuMg_7.

Experimental

Synthesis

Starting materials for the synthesis of RE_3RuMg_7 (RE = Y, Nd, Dy, Ho) were pieces of the rare earth elements

Table 1. Lattice parameters (Guinier powder data) of ternary magnesium compounds with an ordered Ti_6Sn_5-type structure, space group $P6_3/mmc$.

Compound	a (pm)	c (pm)	V (nm^3)	Reference
Y_3RuMg_7	1021.1(2)	608.7(1)	0.5496	this work
Nd_3RuMg_7	1040.7(8)	614.2(4)	0.5761	this work
Sm_3RuMg_7	1034.8(2)	613.00(9)	0.5684	[6]
$Sm_{3.16}RuMg_{6.84}$[a]	1034.1(2)	611.3(1)	0.5661	[6]
Gd_3RuMg_7	1026.4(2)	610.22(6)	0.5568	[6]
Tb_3RuMg_7	1022.3(3)	607.4(2)	0.5497	[6]
Dy_3RuMg_7	1019.1(2)	606.76(9)	0.5457	this work
$Dy_{3.03}RuMg_{6.97}$[a]	1018.97(3)	606.74(2)	0.5456	this work
Ho_3RuMg_7	1016.7(2)	606.2(1)	0.5427	this work

[a] Single crystal data.

(Smart Elements, > 99.9 %), ruthenium powder (Allgemeine Gold- und Silberscheideanstalt, Pforzheim, > 99.9 %) and a magnesium rod (Johnson Matthey, Ø 16 mm, > 99.5 %; the surface of the rod was first cut on a turning lathe in order to remove surface impurities). For the preparation of RE_3RuMg_7 samples pieces of the rare earth elements, ruthenium powder and magnesium were weighed in the ideal atomic ratio of 3 : 1 : 7 and arc-welded [11] in small niobium tubes under an argon pressure of *ca.* 700 mbar. The argon was purified over titanium sponge (900 K), silica gel, and molecular sieves.

The niobium ampoules were sealed in a quartz tube for protection against oxidation and then annealed within 2 h to 1273 K in a muffle furnace. After keeping the temperature for 2 h it was lowered to 673 K within 50 h and kept at 673 K for another 5 h. After cooling by radiative heat loss, the samples were separated mechanically from the ampoules. No reactions with the crucible material were evident.

X-Ray diffraction

The polycrystalline RE_3RuMg_7 samples were first studied through Guinier powder patterns (imaging plate detector, Fujifilm BAS-1800) with Cu$K_{\alpha1}$ radiation and α-quartz ($a = 491.30$, $c = 540.46$ pm) as an internal standard. The hexagonal lattice parameters (Table 1) were deduced from least-squares refinements. Correct indexing of the patterns was ensured by intensity calculations [12]. Only the dysprosium containing sample was obtained in X-ray-pure form for property studies. The other samples showed trace amounts of not yet identified impurity phases.

Single crystals of the dysprosium compound were selected from the annealed sample and glued to thin quartz fibers using beeswax. The crystals were studied on a Buerger camera (using white Mo radiation) to check their quality. The subsequent intensity data collection was performed on a Stoe IPDS-II image plate system (graphite-monochromatized MoK_α radiation; $\lambda = 71.073$ pm) in oscillation mode. A numerical absorption correction was applied to the data set. Details about the data collection and the crystallographic parameters are summarized in Table 2.

Table 2. Crystal data and structure refinement for $Dy_{3.03}RuMg_{6.97}$, space group $P6_3/mmc$, $Z = 2$.

Empirical formula	$Dy_{3.03}RuMg_{6.97}$
Formula weight, g mol^{-1}	762.89
Unit cell dimensions	Table 1
Calculated density, g cm^{-3}	4.64
Crystal size, μm^3	$10 \times 50 \times 50$
Transm. ratio (max / min)	0.391 / 0.840
Absorption coefficient, mm^{-1}	22.2
F(000), e	655
θ range for data collection, deg	2 – 33
Range in hkl	±15, ±15, ±9
Total no. reflections	7658
Independent reflections / R_{int}	439 / 0.0372
Reflections with $I > 2\,\sigma(I)$ / R_σ	373 / 0.0169
Data / parameters	439 / 19
Goodness-of-fit on F^2	0.879
$R1$ / $wR2$ for $I > 2\,\sigma(I)$	0.0109 / 0.0153
$R1$ / $wR2$ for all data	0.0184 / 0.0159
Extinction coefficient	0.00109(9)
Largest diff. peak / hole, e Å^{-3}	0.54 / −0.89

Structure refinement

The diffractometer data set showed a hexagonal lattice with high Laue symmetry, and the systematic extinctions were in agreement with space group $P6_3/mmc$, similar to $Sm_{3.16}RuMg_{6.84}$ [6]. The atomic parameters of the samarium compound were taken as starting values, and the structure was refined with anisotropic displacement parameters for all atoms with SHELXL-97 (full-matrix least-squares on F_o^2) [13, 14]. To check for deviations from the ideal composition, the occupancy parameters were refined in separate series of least-squares cycles. Similar to the $Sm_{3.16}RuMg_{6.84}$ structure, also the dysprosium-containing crystal showed mixing with the rare earth element on the Mg3 site. All other sites were fully occupied within two standard deviations. The Mg3/Dy mixed occupancy was refined as a least-squares variable in the final cycles leading to the composition $Dy_{3.03}RuMg_{6.97}$ for the investigated crystal. The final difference Fourier synthesis revealed no residual peaks. The

Table 3. Atomic coordinates and isotropic displacement parameters (pm^2) for $Dy_{3.03}RuMg_{6.97}$. U_{eq} is defined as one third of the trace of the orthogonalized U_{ij} tensor. Note that the Mg3 site shows mixed occupancy by 97.1(3) % Mg and 2.9(3) % Dy.

Atom	Wyckoff position	x	y	z	U_{eq}
Dy	6*h*	0.12983(1)	2*x*	1/4	100(1)
Ru	2*a*	0	0	0	87(1)
Mg1	6*h*	0.77661(9)	2*x*	1/4	167(3)
Mg2	6*g*	1/2	0	0	142(2)
Mg3	2*c*	1/3	2/3	1/4	190(9)

Table 4. Anisotropic displacement parameters (pm^2) for $Dy_{3.03}RuMg_{6.97}$. The anisotropic displacement factor exponent takes the form: $-2\pi^2[h^2a^{*2}U_{11} + \ldots + 2hka^*b^*U_{12}]$. Note that the Mg3 site shows mixed occupancy by 97.1(3) % Mg and 2.9(3) % Dy.

Atom	U_{11}	U_{22}	U_{33}	U_{23}	U_{13}	U_{12}
Dy	107(1)	96(1)	92(1)	0	0	48(1)
Ru	94(1)	U_{11}	70(2)	0	0	47(1)
Mg1	134(4)	231(7)	168(6)	0	0	115(3)
Mg2	149(4)	164(6)	120(5)	−42(2)	−21(2)	82(3)
Mg3	160(10)	U_{11}	247(13)	0	0	80(5)

refined atomic positions, equivalent isotropic displacement parameters, and interatomic distances are given in Tables 3 and 4.

Further details of the crystal structure investigation may be obtained from Fachinformationszentrum Karlsruhe, 76344 Eggenstein-Leopoldshafen, Germany (fax: +49-7247-808-666; e-mail: crysdata@fiz-karlsruhe.de, http://www.fiz-karlsruhe.de/request_for_deposited_data.html) on quoting the deposition number CSD-426697.

Table 5. Interatomic distances (pm) in $Dy_{3.03}RuMg_{6.97}$ calculated with the single-crystal lattice parameters. Standard deviations are all equal or smaller than 0.4 pm. All distances within the first coordination spheres are listed. Note that the Mg3 site shows mixed occupancy by 97.1(3) % Mg and 2.9(3) % Dy.

Dy:	2	Ru	274.8	Mg1:	4	Mg2	300.2
	2	Mg1	343.0		2	Mg1	336.1
	2	Mg1	345.4		2	Dy	343.0
	1	Mg3	359.2		2	Dy	345.4
	4	Mg2	364.6	Mg2:	4	Mg1	300.2
	4	Dy	380.2		2	Mg2	303.4
	2	Dy	396.9		2	Mg3	331.0
Ru:	6	Dy	274.8		4	Dy	364.6
	2	Ru	303.4	Mg3:	6	Mg2	330.9
					6	Mg1	331.0
					3	Dy	359.2

Physical property measurements

The magnetic property measurements were carried out with a Quantum Design Physical Property Measurement System using a Vibrating Sample Magnetometer. The data collection was performed in the temperature range of 3 – 300 K with flux densities up to 80 kOe (1 kOe = 7.96×10^4 A m^{-1}). 5.203 mg of the polycrystalline sample was packed in a polypropylene capsule and affixed to a brass sample holder rod for the measurements.

Discussion

Crystal chemistry

The magnesium-rich phases RE_3RuMg_7 (RE = Y, Nd, Dy, Ho) extend the recently discovered series of Ti_6Sn_5-type intermetallic magnesium compounds [6]. The course of the cell volumes in the RE_3RuMg_7 series is presented in Fig. 1. As expected from the lanthanoid contraction, one observes a decrease from the neodymium to the holmium compound. The Y_3RuMg_7 cell volume fits between that of the terbium and dysprosium compound as observed for several other isotypic series of $RE_xT_yMg_z$ compounds [1].

The magnesium compounds $RE_3RuMg_7$are ternary ordered variants of the Ti_6Sn_5 type [15] with the *RE*, Ru, Mg1, Mg2, and Mg3 sites corresponding to Ti1, Sn2, Sn1, Ti2, and Sn3. Thus, a simple explanation of the ordering of the elements on the basis of electronegativity trends fails, and the bonding characteristics in the stannide prototype and the magnesium compounds reported here are distinctly different. One should call these phases rather isopointal [16, 17] than isotypic.

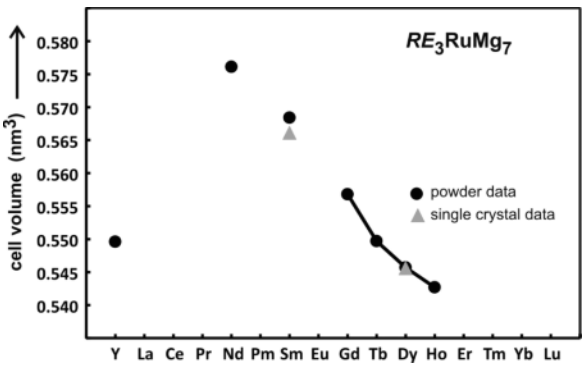

Fig. 1. Course of the cell volumes in the series of hexagonal RE_3RuMg_7 compounds.

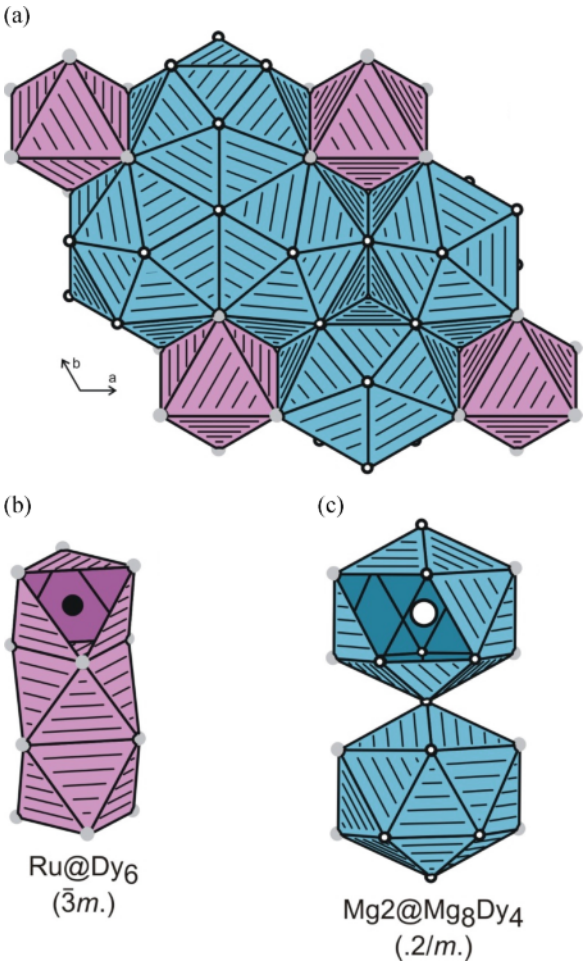

Fig. 2 (color online). a) The crystal structure of Dy_3RuMg_7. Dysprosium, ruthenium and magnesium atoms are drawn as medium grey, black filled and open circles, respectively. The Ru@Dy_6 octahedra (magenta) and Mg2@Mg_8Dy_4 icosahedra (greyish-blue) are emphasized. b) and c) Rows of face-sharing Ru@Dy_6 octahedra and corner-sharing Mg2@Mg_8Dy_4 icosahedra extending along the crystallographic c axis. The site symmetries are indicated.

The following crystal chemical discussion relies on the dysprosium compound for which single crystal data are available. The Dy_3RuMg_7 structure contains two striking polyhedra, ruthenium-centered Ru@Dy_6 octahedra and a distorted icosahedral coordination around the Mg2 atoms (Fig. 2). The Ru@Dy_6 octahedra share common faces, leading to rows that extend along the c axis. Geometrically one can describe the arrangement of these rows as a hexagonal rod packing. These rods are surrounded by six rows of corner-sharing Mg2@Mg_8Dy_4 icosahedra. The packing of these two coordination polyhedra includes all atoms, and one can easily describe the Dy_3RuMg_7 structure this way. Both polyhedra are slightly distorted. Due to the hexagonal symmetry, the ruthenium atoms in the slightly compressed Ru@Dy_6 octahedra have site symmetry $\bar{3}m$ instead of $m\bar{3}m$. Due to the different size of the magnesium and dysprosium atoms, for the coordination shell of the Mg2 atoms the site symmetry is reduced from $\bar{3}m$. to $.2/m$.

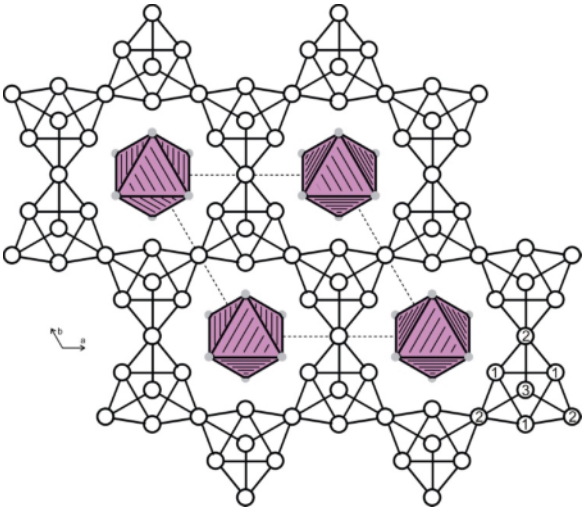

Fig. 3 (color online). Projection of the Dy_3RuMg_7 structure onto the xy plane. Dysprosium, ruthenium and magnesium atoms are drawn as medium grey, black filled and open circles, respectively. The rows of Ru@Dy_6 octahedra and the magnesium substructure are emphasized. The three crystallographically independent magnesium sites are marked at the lower right-hand part.

As expected for a magnesium-rich intermetallic compound, one observes a pronounced magnesium substructure. The Mg–Mg distances of the three crystallographically independent magnesium atoms range from 300 to 336 pm, in close agreement with the average Mg–Mg distance of 320 pm in *hcp* magnesium [18]. Each magnesium atom has between 6 and 12 nearest magnesium neighbors. It is remarkable that the three-dimensional magnesium substructure encapsulates the rows of face-sharing Ru@Dy_6 octahedra (Fig. 3). This way one obtains complete segregation of the two substructures, and consequently there is no Ru–Mg bonding. The Ru–Dy distances of 275 pm are slightly shorter than the sum of the covalent radii of 283 pm [19], indicating strong covalent Ru–Dy bond-

ing. This is similar to the series of RE_4RuMg compounds [3], where the ruthenium atoms are located in condensed trigonal prisms formed by the rare earth atoms.

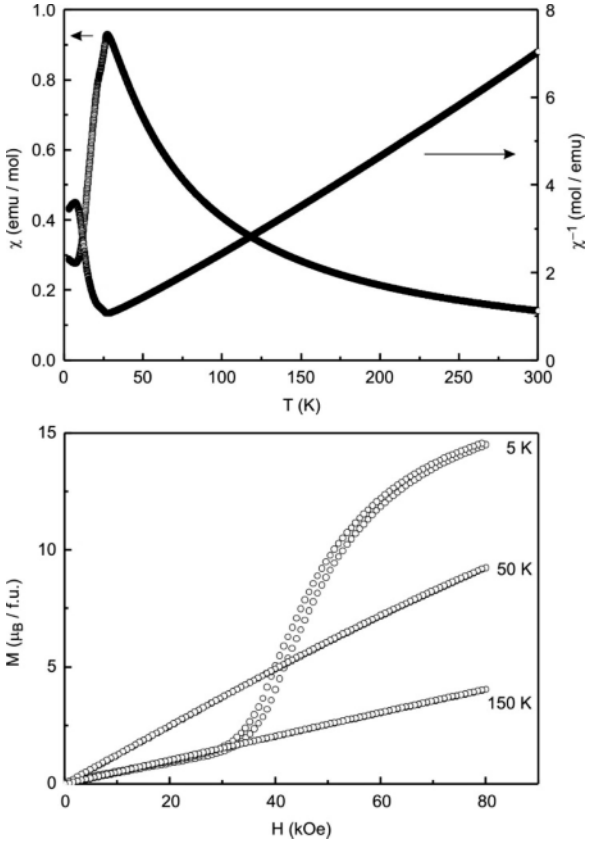

Fig. 4. Temperature-dependent magnetic susceptibility (χ) and inverse magnetic susceptibility data (χ^{-1}) of Dy_3RuMg_7 measured at a magnetic flux density of 10 kOe (top). Magnetization isotherms of Dy_3RuMg_7 measured at 5, 50 and 150 K with magnetic flux densities up to 80 kOe (bottom).

Finally we draw back to the magnesium substructure. Three-dimensional magnesium networks with similar ranges of Mg–Mg distances occur in several other magnesium-rich intermetallic structures, *e. g.* $RETMg_2$ [20], $TbCuMg_4$ [21], $CeRu_2Mg_5$ [8], or $Ce_2Ru_4Mg_{17}$ [9]. However, these magnesium substructures are all bound to the transition metal atoms.

Magnetic properties of Dy_3RuMg_7

The course of the magnetic susceptibility (χ) and the inverse magnetic susceptibility data (χ^{-1}) of Dy_3RuMg_7 is shown in Fig. 4 (top). The inverse magnetic susceptibility data show linear temperature dependence above 150 K, as is expected for a paramagnetic material. The data were fitted with the Curie–Weiss law $\chi = C/(T - \theta_P)$, yielding an effective magnetic moment of $\mu_{eff} = 10.66(1)\ \mu_B$ per Dy atom and a Weiss-constant of $\theta_P = 0.9(5)$ K. Although we observe antiferromagnetic ordering of the compound at $T_N = 27.5(5)$ K, there appears to be almost no long range interactions in the paramagnetic domain.

The magnetization isotherms taken at 5, 50 and 150 K are shown in Fig. 4 (bottom). Both isotherms above the Néel temperature show linear dependence with temperature as expected for a paramagnetic material. The 5 K isotherm, however, exhibits a metamagnetic step at the critical field of $H_C = 40$ kOe while showing a minute hysteresis. The metamagnetic transition manifests the antiferromagnetic ground state of Dy_3RuMg_7. With $M_{max} = 14.6(1)\ \mu_B$ per f. u. less than half of the theoretically possible saturation magnetization [22] is reached for the polycrystalline sample.

Acknowledgement

This work was supported by the Deutsche Forschungsgemeinschaft.

[1] U. Ch. Rodewald, B. Chevalier, R. Pöttgen, *J. Solid State Chem.* **2007**, *180*, 1720.
[2] I. M. Opainich, V. V. Pavyluk, O. I. Bodak, *Crystallogr. Rep.* **1996**, *41*, 813.
[3] S. Tuncel, B. Chevalier, S. F. Matar, R. Pöttgen, *Z. Anorg. Allg. Chem.* **2007**, *633*, 2019.
[4] S. Linsinger, M. Eul, W. Hermes, R.-D. Hoffmann, R. Pöttgen, *Z. Naturforsch.* **2009**, *64b*, 1345.
[5] M. Kersting, O. Niehaus, R.-D. Hoffmann, R. Pöttgen, *Z. Kristallogr.* **2013**, *228*, in press.
[6] S. Linsinger, R. Pöttgen, *Z. Naturforsch.* **2011**, *66b*, 565.
[7] S. Linsinger, U. Ch. Rodewald, R. Pöttgen, *Z. Anorg. Allg. Chem.* **2012**, *638*, 1457.
[8] S. Linsinger, M. Eul, U. Ch. Rodewald, R. Pöttgen, *Z. Naturforsch.* **2010**, *65b*, 1185.

[9] S. Linsinger, R.-D. Hoffmann, M. Eul, R. Pöttgen, *Z. Naturforsch.* **2012**, *67b*, 219.
[10] S. F. Matar, B. Chevalier, R. Pöttgen, *Intermetallics* **2012**, *21*, 88.
[11] R. Pöttgen, Th. Gulden, A. Simon, *GIT Labor-Fachzeitschrift* **1999**, *43*, 133.
[12] K. Yvon, W. Jeitschko, E. Parthé, *J. Appl. Crystallogr.* **1977**, *10*, 73.
[13] G. M. Sheldrick, SHELXL-97, Program for the Refinement of Crystal Structures, University of Göttingen, Göttingen (Germany) **1997**.
[14] G. M. Sheldrick, *Acta Crystallogr.* **2008**, *A64*, 112.
[15] K. Schubert, K. Frank, R. Gohle, A. Maldonado, H. G. Meissner, A. Raman, W. Rossteutscher, *Naturwissenschaften* **1963**, *50*, 41.
[16] L. M. Gelato, E. Parthé, *J. Appl. Crystallogr.* **1987**, *20*, 139.
[17] E. Parthé, L. M. Gelato, *Acta Crystallogr.* **1984**, *A40*, 169.
[18] J. Donohue, *The Structures of the Elements*, Wiley, New York **1974**.
[19] J. Emsley, *The Elements*, Oxford University Press, Oxford **1999**.
[20] M. Kersting, R. Pöttgen, *Z. Naturforsch.* **2011**, *66b*, 651.
[21] P. Solokha, S. De Negri, V. Pavlyuk, A. Saccone, B. Marciniak, *J. Solid State Chem.* **2007**, *180*, 3066.
[22] H. Lueken, *Magnetochemie*, B. G. Teubner, Stuttgart, Leipzig, **1999**.